Poly (N-isopropylacrylamide) microgel-based sensor for progesterone in aqueous samples

Yaxin Jiang[1, 2], Marcos G. Colazo[1*], Michael J. Serpe[2*]

1. Livestock Research Branch, Alberta Agriculture and Forestry, Edmonton, Alberta T6H 5T6, Canada.
2. Department of Chemistry, University of Alberta, Edmonton, Alberta, T6G 2G2, Canada

*Corresponding authors. Tel.: +1 7804159643, Email: marcos.colazo@gov.ab.ca (M. G. Colazo); Tel.: +1 7804925778, Email: michael.serpe@ualberta.ca (M. J. Serpe).

ABSTRACT

Progesterone (P4) is a vital steroid hormone involved in the reproduction cycle and necessary for maintenance of pregnancy in humans and animals. Monitoring P4 concentrations is required in various fields, such as dairy industry, environmental protection and clinical laboratories. The current available methods for P4 determination are either expensive or time consuming. Therefore, more affordable and easy to use sensor technologies for P4 detection are needed. Here, we describe a sensor composed of anti-P4 antibody-modified poly (N-isopropylacrylamide) (pNIPAm) microgels that can be used to construct an optical device (etalon) capable of detecting P4. The binding of P4 and anti-P4 antibodies induces collapse of the pNIPAm microgels in the etalon, resulting in an optical response from the sensor that depends on P4 concentration in solution. Using this developed sensor, a linear detection range of 0.28 ng/mL to 30 ng/mL P4 could be achieved with a detection limit of 0.28 ng/mL and 0.25 ng/mL at room temperature and 30°C, respectively. Moreover, the sensor showed low cross-reactivity with 17β-estradiol (E2), demonstrating that the sensor can be used to quantify P4 in the presence of the interference E2.

KEYWORDS

Progesterone sensing, Biosensor, Poly (N-isopropylacrylamide) microgels, Stimuli responsive polymers, Etalons

INTRODUCTION

Progesterone (P4; also known as pregn-4-ene-3, 20-dione) is a 21-carbon steroid hormone, which plays a critical role in establishing and maintaining the mammalian reproductive system [1]. An imbalance of P4 levels in mammals can cause malformations in the reproductive system as well as infertility [2]. High levels of P4 in humans may result in mood swings, anxiety and body pain in women [3], as well as abnormal behavior in men due to the decreased release of testosterone [4]. In clinical medicine, P4 has been used as hormone therapy for the treatment of gender identity disorder (GID) in children and adolescents [5]. However, the human body may only partially absorb P4, with the excess being released as waste to sewage treatment facilities and subsequent release into the environment. The continuous release of P4 into the environment can also lead to health problems in wild animals, especially with fish and other aquatic life. Therefore, it is important to monitor P4 concentration in environmental samples to protect the environment and human health [6]. It is also of utmost importance to monitor the concentration of P4 in biological fluids in dairy cows, which can be used to detect estrus. Accurate estrus detection can ultimately lead to improved reproductive efficiency in dairy herds, improved cow health, and increased profits for farmers [7]. Estrus is preceded by a reduction in P4 and an increase in estradiol (E2) levels [8]. Hence, by monitoring the level of these hormones in blood or milk it is possible to predict when a cow will be in estrus and will allow the cow to be inseminated at the optimal time [9, 10]. Therefore, the determination of progesterone concentration has attracted the dairy industry's interest. While this is the case, the purpose of this submission is to demonstrate that P4 sensors can be generated, by investigating their performance in aqueous samples. The results will then be used to develop a sensor for P4 in milk samples.

Numerous methods have been developed for quantifying the amount of P4 in various samples [6, 11-20]. For example, radioimmunoassay (RIA) is an analytical method often used to determine P4 concentration in a rapid fashion with high sensitivity [11]. However, it requires specialized and expensive facilities and involves the use of radioactive materials, which have serious environmental concerns.

Conversely, enzyme-linked immunosorbent assays (ELISA) for P4 determination uses antibody-enzyme conjugates instead of radioactive materials [12], but it requires considerable time to obtain a result and ELISA kits are still prohibitively expensive. Recently, sensitive advanced instrumental methods, such as high-performance liquid chromatography (HPLC), liquid chromatography/mass spectroscopy (LC/MS) or gas chromatography/mass spectroscopy (GC/MS), have been developed to quantify P4 [13, 14]. All of these approaches require considerable time for sample preparation and analysis, are expensive, and need highly trained personnel and a lab environment — therefore, they are not suited for field measurements. Additionally, numerous biosensors have been developed in recent years to monitor hormones in clinical, pharmaceutical, environmental, and dairy samples [6, 15-20]. In one example, electrochemistry-based progesterone immunosensors were generated from nanostructured materials, and were shown to be able to quantify P4 in milk [16] and serum [17] samples. However, enzyme-labeled progesterone (like ELISA) was needed to generate the signal [16, 17], which makes these methods expensive, complicated, and they have a short shelf-life. Several optical biosensors have also been developed to detect P4 concentrations using various techniques and materials. For example, quantum dot-based immunoluminescent sensors have been developed that are capable of detecting progesterone concentration in the range of 0.3 to 14.5 ng/mL in 10-fold diluted cow milk [18]. Total internal reflectance fluorescence (TIRF)-based approaches have also been developed that can achieve a limit of quantitation (LOQ) of 0.34 ng/mL [19]. Finally, a surface plasmon resonance (SPR) spectroscopy-based approach has been shown to detect P4 concentration as low as 3.5 ng/mL P4 [20].

In our previous investigations, we showed that stimuli-responsive polymer-based systems could be generated and used for a variety of applications [21-24]. Stimuli-responsive polymers have the ability to respond physically and/or chemically in response to environmental changes [25, 26]. Among these stimuli-responsive polymers, thermoresponsive poly (N-isopropylacrylamide) (pNIPAm), has attracted the most

attention [27]. PNIPAm has a lower critical solution temperature (LCST) of 32 °C where it undergoes a conformational change from an extended random coil to a collapsed globule [27]. PNIPAm-based hydrogel particles (microgels) can also be synthesized, and exhibit thermoresponsivity, i.e., they decrease in diameter above 32 °C. PNIPAm-based microgels have been used for myriad applications, e.g., sensors, catalysts, drug delivery platforms, water remediation materials and artificial tissues [21-24, 28-30]. In this submission, pNIPAm-*co*-acrylic acid (pNIPAm-*co*-AAc) microgels were used to generate optical device (etalons) and were made sensitive to the concentration of P4 in water samples. Figure 1A shows the basic structure of the etalon, which is composed of two semi-transparent metal layers (Au in our case) "sandwiching" a layer of pNIPAm-based microgels, all on a glass support. These devices also exhibit visual color and multipeak reflectance spectra, as can be seen in Figure 1B. The wavelength(s) of light reflected from the etalons can be predicted from Equation (1):

$$\lambda = \frac{2nd\cos\theta}{m} \qquad (1)$$

where n is the refractive index of the dielectric (microgel) layer, d is the distance between the metal layers, θ is the angle of incident light relative to the device normal, and m is the order of a reflected wavelength (an integer). For our devices, we have shown that the position of the peaks in reflectance spectra (and hence the device color) depends primarily on the distance between the metal layers. Since the devices are composed of responsive microgels, they can be used to modulate the metal layer separation, which leads to shifts in the peaks in the reflectance spectra and a device that exhibits color tunability. Microgels can be made responsive to multiple stimuli by modifying their chemistry, allowing the devices to detect multiple stimuli by monitoring their optical properties. In this investigation, we modified pNIPAm-based microgels with polyclonal progesterone antibodies, as shown schematically in Figure 1A, which were used to quantify P4 in water samples. The sensing mechanism relies on antibody crosslinking in the presence of P4, which causes the microgels to collapse, leading to a change in the optical properties (blue shift) of the device. By

monitoring the shift of the reflectance peaks, a P4 sensor could be generated that is inexpensive, easy to use, and capable of quantifying the concentration of steroid hormones in water and wastewater.

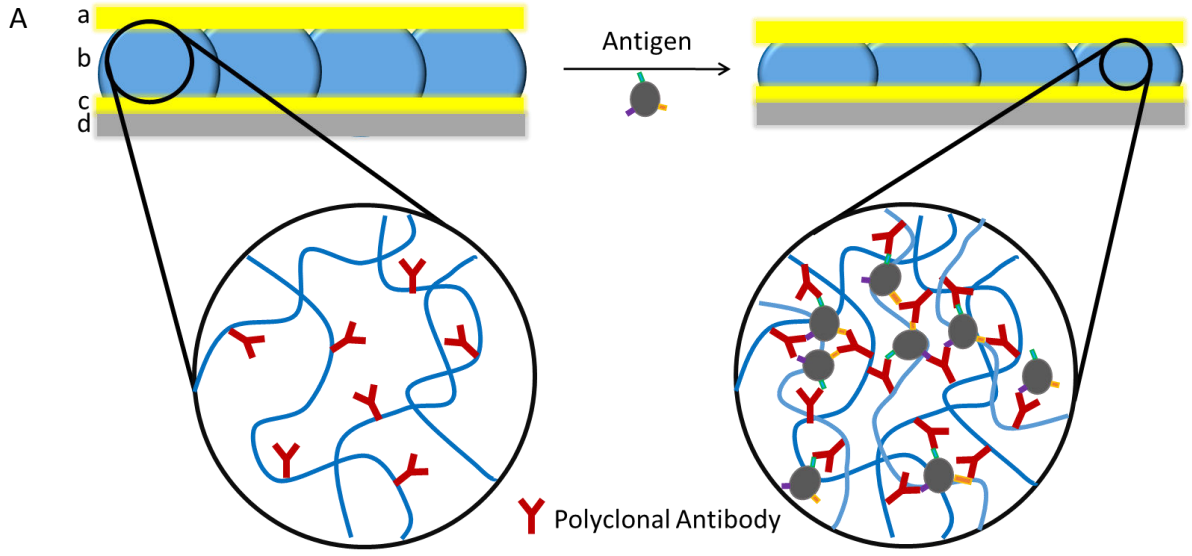

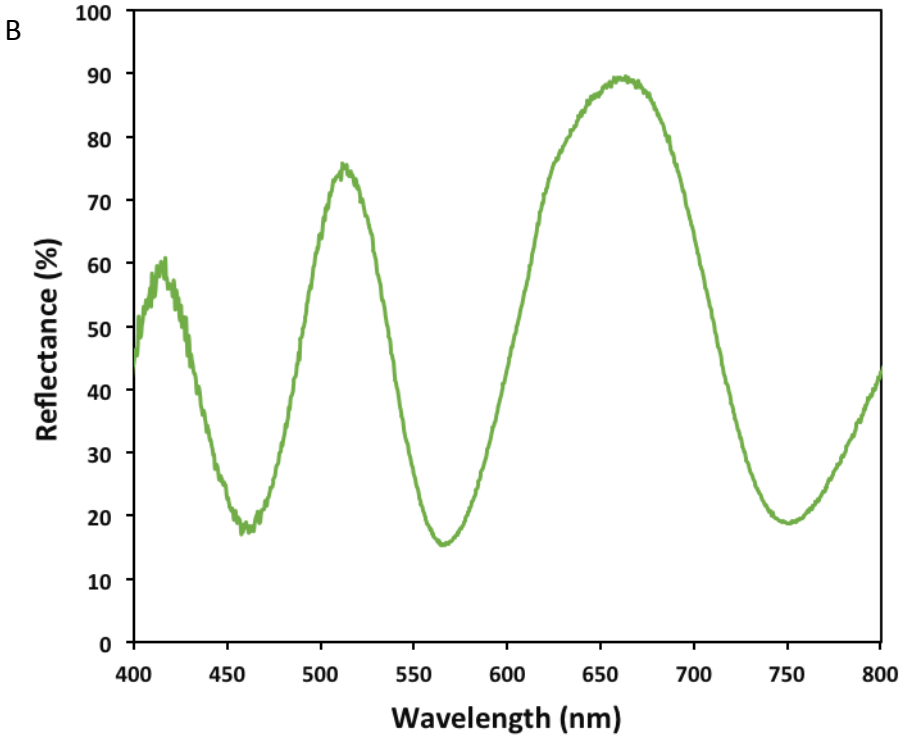

Figure 1. (A, left) Schematic of an etalon, where (a) and (c) are 15 nm Au layers (with 2 nm Cr as adhesion layer) sandwiching a (b) microgel layer (d) all on a glass substrate. (A) Also shows the sensing mechanism,

with microgel-bound antibodies binding the P4 antigen, and becoming crosslinked, leading to a collapse in the microgel layer. (B) A reflectance spectrum obtained from a typical etalon used in this investigation.

EXPERIMENTAL SECTION

1. Materials

N-Isopropylacrylamide (NIPAm) was purchased from TCI (Portland, OR, USA) and purified by recrystallization from hexanes (ACS reagent grade, EMD, Gibbstown, NJ, USA) prior to use. N, N-methylenebisacrylamide (BIS) (99%), acrylic acid (AAc) (99%), ammonium persulfate (APS) (>98%), 1-ethyl-3-(3-dimethylaminopropyl) carbodiimide hydrochloride (EDC), N-hydroxysuccinimide (NHS), progesterone, and 17β-estradiol were purchased from Sigma-Aldrich (Oakville, ON, Canada) and used as received. Phosphate buffer saline (PBS, 10 mM, pH 7.4) was purchased from Fisher Scientific (Ottawa, ON, Canada), and deionized (DI) water with a resistivity of 18.2 MΩ·cm was used in all experiments. The 25 × 25 × 1 mm glass coverslips were obtained from Fisher Scientific. Au (99.99 %) was obtained from MRCS Canada (Edmonton, AB). Cr (99.999 %) was obtained from ESPI (Ashland, OR, USA). Two polyclonal anti-progesterone antibodies were used in this research. Rabbit polyclonal anti-progesterone antibody (antibody A) was purchased from Novus (Oakville, ON, Canada), and sheep polyclonal anti-progesterone antibody (antibody B) was purchased from Pierce Antibodies (Ottawa, ON, Canada). Experiments were conducted at room temperature (21 ± 1 °C) unless otherwise specified.

2. Microgel Synthesis

Poly (N-isopropylacrylamide-*co*-acrylic acid) (pNIPAm-*co*-AAc) microgels were synthesized via temperature-ramp, surfactant-free, free-radical precipitation polymerization as described previously [31, 32]. Briefly, the monomer mixture was composed of 85% NIPAm and 10% AAc with 5% BIS as a crosslinker. First, NIPAm (11.9 mmol), and BIS (0.7 mmol) were dissolved in deionized water (99 mL) with stirring in a beaker. The mixture was filtered into a 200 mL 3-neck round bottom flask through a 0.2 μm filter. The

solution was bubbled with N_2 gas for ~1.5 h while allowing the temperature to reach 70 °C. AAc (1.4 mmol) was then added to the heated mixture followed by the addition of 1 mL of 0.2 M aqueous solution of the initiator APS. The reaction was allowed to proceed for 4 hours at 70 °C and the reaction mixture was stirred overnight at room temperature. The mixture was finally filtered through glass wool to remove any large aggregates, and were washed to remove unreacted monomer and linear polymer by centrifugation (~8500 rcf) and resuspension in DI water a total of six times.

3. Etalon Fabrication

A previously described "paint-on" protocol was used to fabricate microgel-based etalons [33]. Briefly, 2 nm of Cr (for adhesion) followed by 15 nm of Au was thermally evaporated onto 25 × 25 × 1 mm glass coverslips (pre-cleaned by rinsing with DI H_2O and ethanol and dried with N_2 gas) at a rate of ~0.1 and ~0.15 Å s^{-1}, respectively, using a model THEUPG thermal evaporation system (Torr International Inc., New Windsor, NY). The Au coated substrates were annealed at 250 °C for 2 h using a Thermolyne muffle furnace from Thermo Fisher Scientific (Ottawa, Ontario). A 40 µL aliquot of concentrated pNIPAm-*co*-AAc microgels (obtained by centrifugation) was spread on the Au/Cr coated substrate according to the "paint-on" protocol [33]. The microgel solution was allowed to dry completely on the substrate for 2 h at 35 °C. Then the dry film was rinsed copiously with DI water to remove any excess microgels not bound directly to the Au. The substrate was then placed into a DI water bath and allowed to incubate overnight at 30 °C. Following this step, the substrate was rinsed again with DI water, dried with N_2 gas, and an additional layer of 2 nm Cr and Au (either 15 nm or 5 nm thick) was deposited.

4. Microgel-Antibody Coupling Reaction

EDC-NHS [34] was used to chemically attach the antibodies to the pNIPAm-*co*-AAc microgels. In detail, pNIPAm-*co*-AAc microgel-based etalons were soaked in PBS, and incubated with a 2 mL mixture of 100 mM EDC and 100 mM NHS for 1 h at room temperature. The etalons were washed copiously with PBS

buffer to remove any unreacted EDC and NHS. The activated etalons were further incubated with 50 µg/mL anti-progesterone antibodies at room temperature for 4 h. The etalons were then washed copiously with PBS buffer to remove any unreacted antibodies. The antibody modified etalons were stored in PBS at 4°C until used. Control devices were prepared by performing the procedure above without EDC and NHS addition.

5. Reflectance Spectroscopy, Optical Microscopy, and Zeta Potential Measurements

Reflectance spectroscopy measurements were performed using a USB2000+ spectrophotometer, a HL-2000-FHSA tungsten light source, and a R400-7-VIS-NIR optical fiber reflectance probe from Ocean Optics (Dunedin, FL). The spectra were collected using OceanView Spectroscopy Software in a wavelength range of 350−1000 nm. Optical microscopy images of the pNIPAm-*co*-AAc microgels were taken using an Olympus IX71 inverted microscope (Markham, Ontario) fitted with a 100X oil-immersion objective an Andor Technology iXon camera (Belfast, Ireland). Andor SOLIS v4.15.3000.0 software was used to record microscopy images of the microgels. Zeta potential and microgel diameter was measured using a Malvern Zetasizer Nano ZS instrument (Malvern, UK) with a 633 nm laser at 25 °C.

6. Experimental setup and sensing procedure

Experiments were done in a custom built chamber with temperature control. The chamber was built to ensure that the position of the etalon and the light source are fixed, and the temperature is well controlled and stable. The chamber allowed the reflectance probe to be inserted such that the device's optical properties could be assessed. The intensity and distance of light source from the assembly was adjusted to result in the highest quality reflectance spectra. During the sensing experiments, the reflectance spectra were collected before adding target and 30 minutes after adding various concentrations of target.

RESULTS AND DISCUSSION

1. Microgel Characterization

Optical microscopy was used to collect images of synthesized pNIPAm-*co*-AAc microgels. Figure 2 shows differential interference contrast (DIC) images of microgels synthesized for this investigation. As can be seen from the image, the microgel diameters are in the range of 1.0 µm-1.2 µm. Dynamic light scattering (DLS) revealed that the average microgel diameter was 1120 ± 30 nm, which is comparable to that measured via microscopy. Zeta potential was also used to characterize the microgels. The pKa of AAc is ~4.25, therefore, the microgels should be negatively charged at pH > pKa. Microgels dispersed in DI water exhibited a zeta potential of -32 ± 1 mV, while they exhibited a zeta potential of 0.06 ± 0.06 mV after coupling with anti-progesterone antibodies (Supplemental Information Figure S1). This suggests that the anti-progesterone antibodies were able to couple to the microgel COOH groups. Previous research has shown that there is a higher concentration of –COOH in the "inner" regions of pNIPAm-*co*-AAc microgels relative to the "outer" regions [35]. Moreover, the size of the antibodies is in the range of 5-10 nm. Therefore, we expect that the antibodies are small enough to penetrate the microgels to couple to the –COOH groups inside the microgels. Considering the concentration of antibodies used, and the density of –COOH in the microgels, ~19,000 antibodies could be coupled to each microgel at 10 % reaction efficiency.

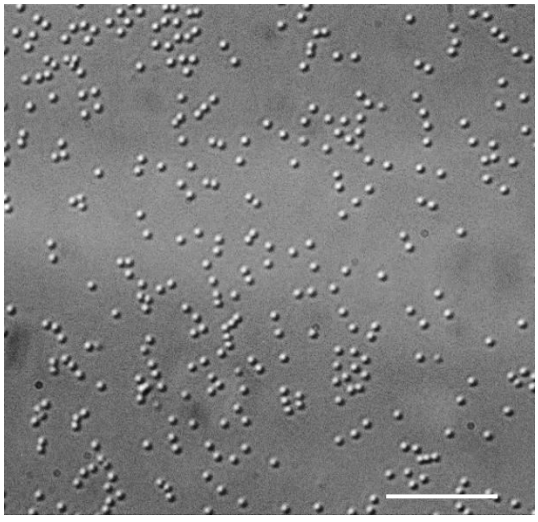

Figure 2. DIC optical microscopy image of pNIPAm-co-AAc microgels used in this investigation, the scale bar is 20 µm.

2. Etalon Fabrication and P4 Detection — Antibody A Modification

The "paint-on" method [33] was utilized to form a monolayer of pNIPAm-*co*-AAc microgels on a glass substrate coated with 2 nm of Cr followed by 15 nm of Au. In previous research, the thermo- and pH-responsivity of pNIPAm-*co*-AAc microgels was reported, and is well documented [36, 37]. Therefore, the etalons constructed here from pNIPAm-*co*-AAc microgels should also show responsivity to temperature and pH [32, 38]. To confirm that our microgels and etalons behave as expected, their response of the fabricated etalons to pH and temperature was analyzed. Analysis revealed that the etalons exhibited the expected behavior — a blue shift of etalon's reflectance peaks was observed when their temperature was increased and when the solution pH was decreased. Likewise, a red shift of the reflectance peaks were observed when the solution temperature was decreased and/or the solution pH was increased (Supplemental Information Figure S2).

With the basic etalon responsivity confirmed, we moved on to evaluate the devices ability to detect P4. Initially, progesterone antibody A-modified microgel-based devices were fabricated and their response to P4 investigated. Figure 3(A) shows that the position (λ_{max}) of the monitored reflectance peak shifts as the device is exposed to various P4 concentrations. Figure 3(B) shows the average peak shift ($\Delta\lambda$) of three devices to various P4 concentrations. As can be seen, the maximum peak shift was ~50 ± 20 nm in response to 50 ng/mL P4. A linear range up to 20 ng/mL was obtained, and the response could be described by Equation (2) with R^2 = 0.9869:

$$\Delta\lambda = 1.68\ (\pm 0.28)\ C_{P4} + 2.02\ (\pm 0.42) \qquad (2)$$

207 Thus, the sensor developed here can be used to measure P4 concentration in aqueous solutions, and can
208 impact environmental monitoring efforts. A detection limit of 3.6 ng/mL was calculated based on three
209 times of standard deviation of blank samples.

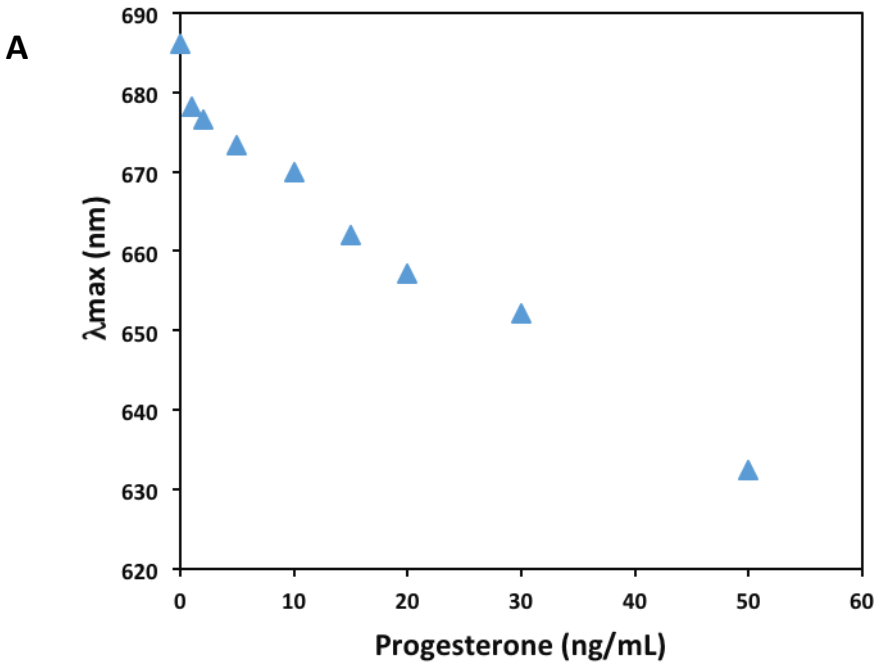

210

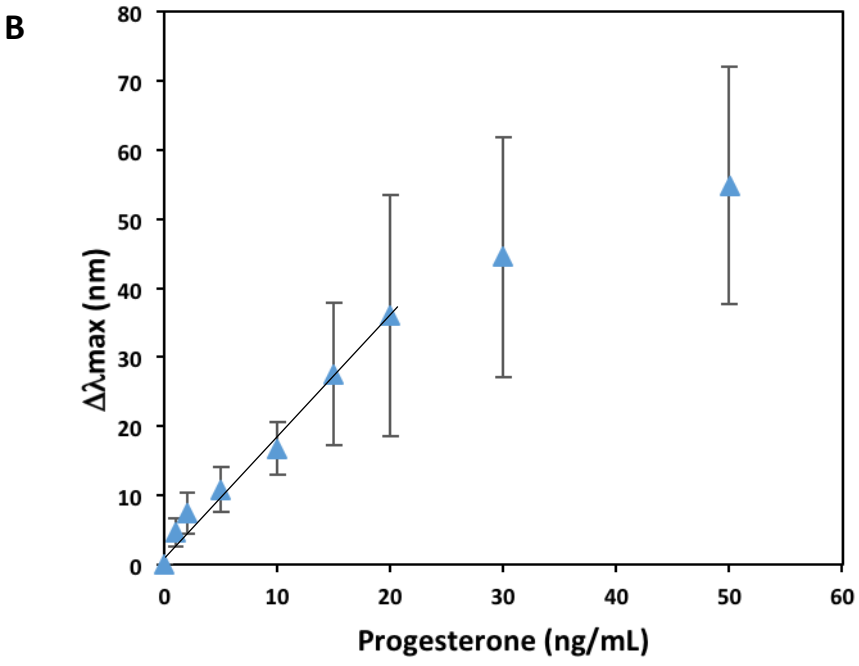

211

Figure 3. (A) The position of a given reflectance peak as a function of P4 concentration. (B) Cumulative shifts of the etalon's reflectance peak for the addition of progesterone to the etalon at room temperature. The peak shifts were calculated relative to the initial peak position. Each data point represents the average of at least three independent measurements, and the error bars are the standard deviation for those values.

3. Effect of Au Overlayer Thickness on Device Sensitivity to P4

The thickness of an etalon's Au overlayer has been shown to significantly impact the transportation of molecules from solution into etalon [39]. Specifically, thin Au has big pores, which we hypothesize will favor the transportation of P4 antibodies and P4 into the etalon, and lead to enhanced sensitivity. To investigate this, we determined the response of a device composed of a 5 nm Au overlayer, and compared that to the response from a device composed of a 15 nm Au overlayer. The results can be seen in Figure 4. As can be seen, the device composed of a 5 nm Au overlayer showed a response of 42 ± 7 nm when exposed to 50 ng/mL P4. Comparably, the device composed of a 15 nm Au overlayer exhibited a response of 50 ± 20 nm when exposed to the same P4 concentration (data shown above). As can be seen, the overall sensitivity of the device to P4 was not significantly affected, although the precision was greatly enhanced for the device with the 5 nm Au overlayer. Additionally, the linear range of the 5 nm Au overlayer device was much larger than the 15 nm Au overlayer device — 0-50 ng/mL P4. The equation that fits the 5 nm Au overlayer data can be seen in Equation (3) with an $R^2 = 0.9531$:

$$\Delta\lambda = 0.80\ (\pm 0.26)\ C_{P4} + 5.11\ (\pm 2.86) \qquad (3)$$

A detection limit of 1.77 ng/mL was also calculated for the 5 nm Au overlayer devices using three times the standard deviation of blank samples. This sensitivity is also improved compared to the 15 nm Au overlayer devices.

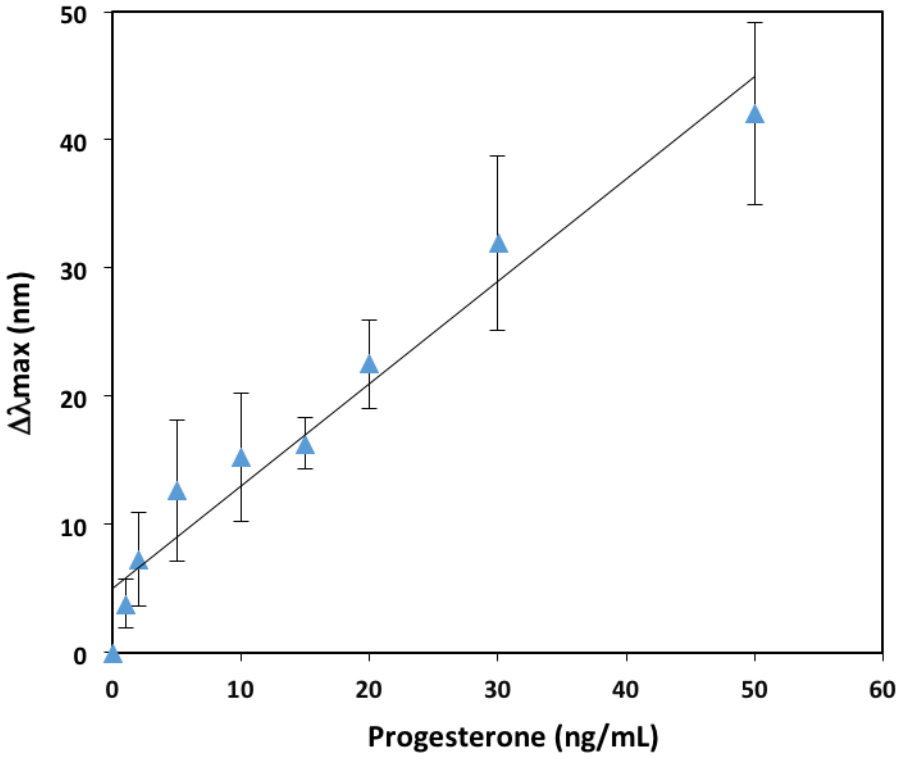

Figure 4. Reflectance spectrum peak shift of antibody A-modified etalons with a Au overlayer thickness of 5 nm as a function of P4 concentration at room temperature. The peak shifts were calculated relative to the initial peak position. Each data point represents the average of at least three independent measurements, and the error bars are the standard deviation for those values.

4. Effect of Temperature on Device Sensitivity to P4

Previously, we have shown that our etalons change their optical properties in response to temperature, and are especially sensitive in the region around the LCST. That is, a blue shift of the devices reflectance peaks is observed as the temperature approaches 32 °C, and is extremely sensitive in the range of 30-34 °C [40]. Therefore, the devices response to other stimuli should exhibit enhanced sensitivity near this transition temperature. We investigated the response of the sensors (5 nm Au overlayer) to different P4 concentrations at 30 °C (Figure 5). As can be seen, the response to 50 ng/mL P4 was 55 ± 7 nm, which is not significantly different to that at room temperature (42 ± 7 nm, P= 0.14 at 95% confidence). Additionally,

two linear ranges were obtained with these devices, from up to 30 ng/mL and above 30 ng/mL is described by Equation (4) and Equation (5), respectively.

$$\Delta\lambda = 6.02\ (\pm 0.36)\ C_{P4} + 0.24\ (\pm 0.12) \quad (4)$$

$$\Delta\lambda = 1.08\ (\pm 0.0.13)\ C_{P4} + 15.34\ (\pm 1.67) \quad (5)$$

A detection limit of 0.25 ng/mL was also calculated for the 5 nm Au overlayer devices at 30 °C using three times the standard deviation of blank samples. The results suggest that the sensor has two different sensitivities in two separate linear ranges. Specifically, the sensor response to P4 is more sensitive at lower concentration. Finally, the response of an etalon to P4 concentration at 40 °C was also was investigated, which exhibited a low sensitivity of 16 ± 6 nm. This diminished sensitivity is likely the result of the microgels in the device being collapsed, and hence cannot respond by deswelling any further upon P4 addition. Therefore, we determined that the sensor has the highest sensitivity at 30 °C, although the device is still functional at room temperature, capable of quantifying P4 in the range of 1.77 ng/mL to 50 ng/mL. These results demonstrate that the device could find real-world applications.

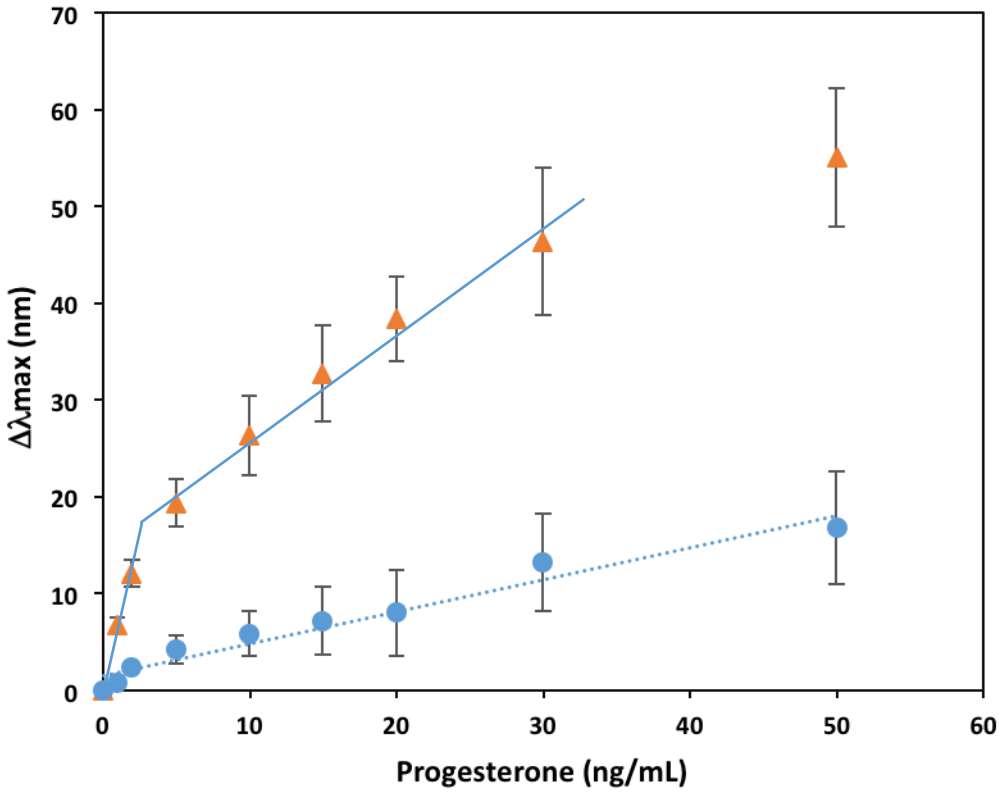

259

260 Figure 5. Reflectance spectrum peak shifts of antibody A-modified etalons with a Au overlayer thickness of
261 5 nm as a function of P4 concentration at (▲) 30 °C and at (●) 40 °C. The peak shifts were calculated
262 relative to the initial peak position. Each data point represents the average of at least three independent
263 measurements, and the error bars are the standard deviation for those values.

264

265 **5. Specificity of the P4 Sensor**

266 The specificity of the devices for P4 was determined by exposing the devices to 17β-estradiol,
267 which is a common interfering species. As can be seen in Figure 6A, the devices showed a maximum
268 response of 11 ± 2 nm (room temperature) and 12 ± 1 nm (30 °C) to 50 ng/mL estradiol; which is
269 significantly lower than the etalons' response to 50 ng/mL progesterone, 42 ± 7 nm (room temperature)
270 and 55 ± 7 nm (30 °C). The ratio of the etalon's sensitivity (slopes of the lines in the calibration curves)

toward progesterone: estradiol is 3.6 (room temperature) and 30.3 (30 °C), which demonstrates that this device can be used to effectively quantify progesterone in the presence of estradiol. We also performed a control experiment, by exposing a device composed of microgels with no progesterone antibodies covalently attached to the microgels in the devices. That is, the microgels were exposed to progesterone antibodies without EDC and NHS addition. Figure 6B shows the response of the control etalon device to different P4 concentrations at room temperature and 30 °C. The control sensors showed 24 ± 10 nm and 12 ± 14 nm peak shift at room temperature and 30 °C, respectively; which also are significantly lower than the obtained 42 ± 7 nm (room temperature) and 55 ± 7 nm (30 °C) of those sample etalon sensors. This result indicates that the physical absorption of antibody in microgels was low, which yielded a decreased response to P4.

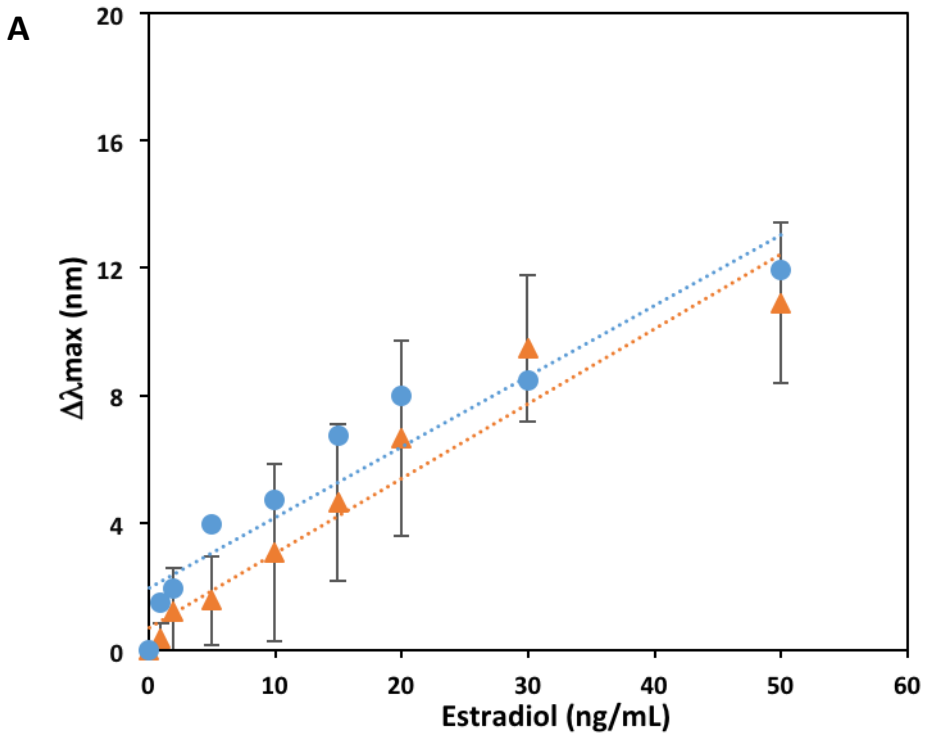

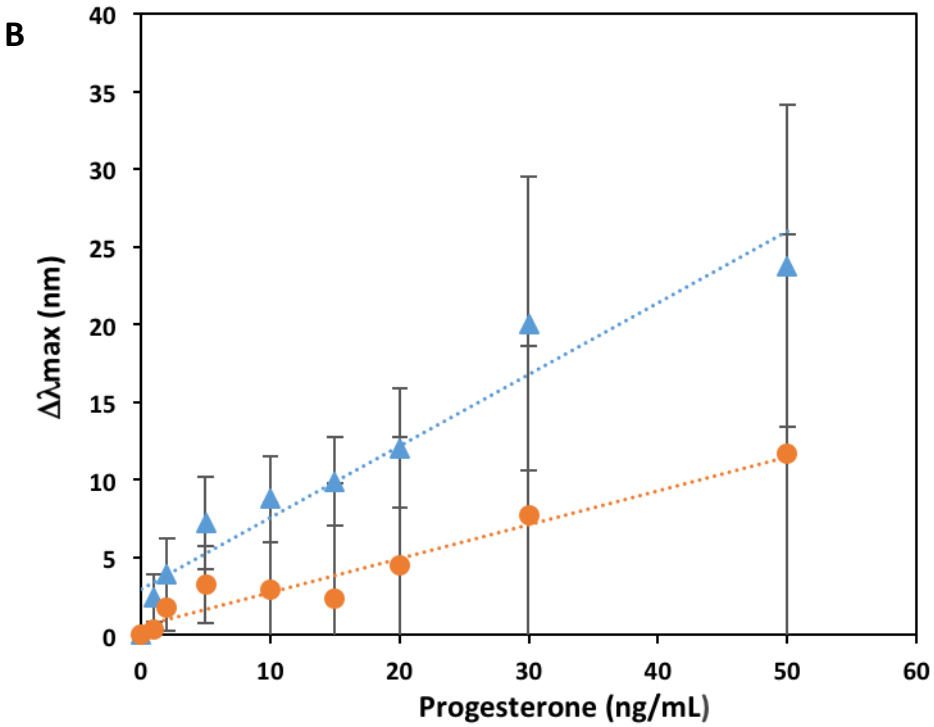

Figure 6. (A) Reflectance spectrum peak shifts of antibody A-modified etalons with a Au overlayer thickness of 5 nm as a function of estradiol concentration at (▲) room temperature and at (●) 30 °C. The peak shifts were calculated relative to the initial peak position. (B) Reflectance spectrum peak shifts of control etalons with a Au overlayer thickness of 5 nm as a function of progesterone concentration at (▲) room temperature and at (●) 30 °C. The peak shifts were calculated relative to the initial peak position. Each data point represents the average of at least three independent measurements, and the error bars are the standard deviation for those values.

6. Etalon Fabrication and P4 Detection -- Antibody B Modification

The above results were obtained with antibody A-modified devices, which exhibited good performance. To confirm the utility of the etalon-based sensor technology, sheep polyclonal progesterone antibody (antibody B) was also coupled to microgels in the etalon, and the response of these devices to

296 different P4 concentrations were tested at room temperature and 30 °C. As can be seen in Figure 7, the
297 results are similar to what was obtained with the etalons modified with antibody A. Two linear ranges were
298 also obtained with these devices, at low and high concentration. Equation (6) (R^2=0.9931) and Equation (7)
299 (R^2=0.9472) (room temperature) and Equation (8) (R^2=0.987) and Equation (9) (R^2=0.9963) (30 °C) describes
300 the response in above concentration respectively:

301 $$\Delta\lambda = 5.32\ (\pm 0.38)\ C_{P4} + 0.25\ (\pm 0.12) \quad (6)$$

302 $$\Delta\lambda = 0.50\ (\pm 0.08)\ C_{P4} + 14.41\ (\pm 1.66) \quad (7)$$

303 $$\Delta\lambda = 3.66\ (\pm 0.36)\ C_{P4} + 0.24\ (\pm 0.12) \quad (8)$$

304 $$\Delta\lambda = 1.00\ (\pm 0.03)\ C_{P4} + 9.96\ (\pm 0.40) \quad (9)$$

305 Detection limits of 0.28 ng/mL (room temperature) and 0.30 ng/mL (30 °C) were calculated using three
306 times the standard deviation of blank samples. The sensors also are also more sensitive at the low
307 concentration range. Successful detection of progesterone using antibodies from different species further
308 confirmed the ability of the sensors to detect steroid hormones.

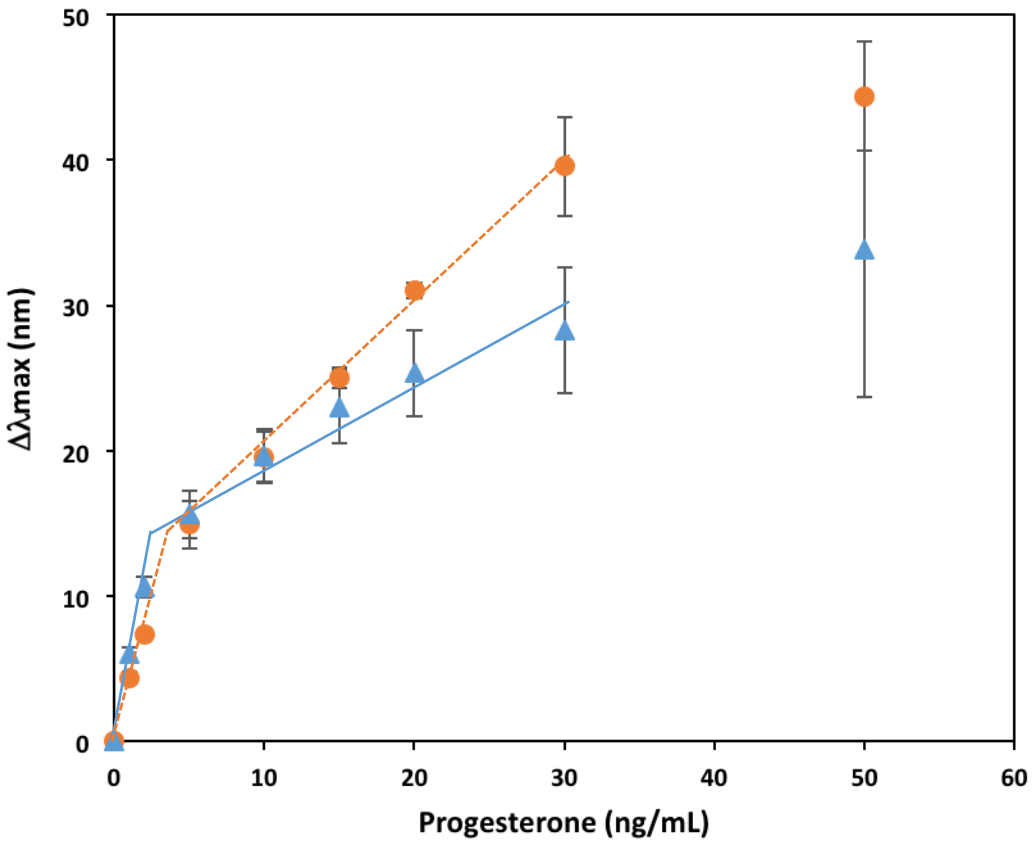

309

310 Figure 7. Reflectance spectra peak shift of polyclonal anti-progesterone antibody B modified etalon with Au
311 overlayer thickness of 5 nm under different concentration of progesterone at (▲) room temperature and
312 at (●) 30 °C. Each data point represents the average of at least three independent measurements, and the
313 error bars are the standard deviation for those values.

314

315 **CONCLUSION**

316 In this submission, we described a device capable of quantifying P4 in aqueous solutions by modifying
317 microgels in etalons with two different P4 antibodies. The ability of the sensors to detect different P4
318 concentrations was determined by monitoring the position of the reflectance peaks in the devices
319 reflectance spectra. We showed that the devices could be used over a wide range of P4 concentrations,

with a detection limit of 0.28 ng/mL and 0.25 ng/mL at room temperature and 30 °C respectively. The devices also exhibited good selectivity in the presence of the common interfering species 17β-estradiol. While these devices could find use as sensors for P4 concentration in aqueous samples, they could also be easily modified to determine the concentration of P4 in milk samples, which can help the dairy industry tremendously. The concept could also be used to determine the concentration of other antigens in samples, which could be used for disease diagnostic applications. Finally, the cost of each device was estimated to be ~ \$4 CAD/inch^2 with over 97% of the cost coming from the purchase of antibodies. We expect to cut this cost further by purchasing components in bulk, making this sensing technology feasible for real-world sensing applications.

ACKNOWLEDGEMENT

MJS acknowledges funding from the University of Alberta (the Department of Chemistry and the Faculty of Science), the Natural Sciences and Engineering Research Council of Canada (NSERC), the Canada Foundation for Innovation (CFI), the Alberta Advanced Education & Technology Small Equipment Grants Program (AET/SEGP), Grand Challenges Canada, and IC-IMPACTS. Funding from *Growing Forward 2,* a federal-provincial-territorial initiative, and Alberta Agriculture and Forestry is also acknowledged.

Compliance with Ethical Standards: Authors declare no financial or non-financial conflicts of interest.

REFERENCES

[1]. Baulieu E, Schumacher M, (2000) Progesterone as a neuroactive neurosteroid, with special reference to the effect of progesterone on myelination, Steroids. 65: 605-612

[2] King TL, Brucker MC, (2010) Pharmacology for Women's Health, 1st ed.; Jones & Bartlett Publishers: San Francisco, CA; pp. 372

[3] Sherwin BBJ, Progestogens used in menopause. Side effects, mood and quality of life, (1999) J. Reprod. Med. 44:227–232

[4] Schneider JS, Stone MK, Wynne-Edwards KE, Horton TH, Lydon J, O'Malley B, Levine JE, (2003) Progesterone receptors mediate male aggression toward infants, Proc. Natl. Acad. Sci. U.S.A. 100:2951–2956

[5] Hewitt JK, Campbell P, Porpavai K, Grover SR, Newman LK, Warne GL, (2012) Hormone treatment of gender identity disorder in a cohort of children and adolescents, Med. J. Aust. 196:578–581

[6] Jimenez GC, Eissa S, Ng A, Alhadrami H, Zourob M, Siaj M, (2015) Aptamer-based label-free impedimetric biosensor for detection of progesterone, Anal. Chem. 87:1075−1082

[7] Ambrose DJ, and Colazo MG, (2007) Reproductive status of dairy herds in Alberta: a closer look, WCDS Adv. Dairy Technol. 19:227-244

[8] Hart JP, Pemberton RM, Luxton R, Wedge R, (1997) Studies towards a disposable screen-printed amperometric biosensor for progesterone, Biosens. Bioelectron. 12:1113-1121

[9] Dobson H, Midmer SE, Fitzpatrick R, (1975) Relationship between progesterone concentrations in milk and plasma during the bovine oestrous cycle, J. Vet Rec. 96:222–223

[10] Colazo MG, Ambrose DJ, Kastelic JP, Small JA, (2008) Comparison of 2 enzyme immunoassays and a radioimmunoassay for measurement of progesterone concentrations in bovine plasma, skim milk, and whole milk, Can. J. Vet. Res. 72:32-36

[11] Capparelli R, Iannelli D, Bordi AJ, (1987) Use of monoclonal antibodies for radioimmunoassay of water buffalo milk progesterone, Dairy Res. 54:471−477.

[12] Shrivastav TG, Chaube SK, Rangari K, Kariya KP, Singh R, Nagendra A, (2010) Enzyme linked immunosorbent assay for milk progesterone, Immunoassay Immunochem. 31:301−313

[13] Beiraghi A, Pourghazi K, Amoli-Diva M, (2014) Au nanoparticle grafted thiol modified magnetic nanoparticle solid phase extraction coupled with high performance liquid chromatography for determination of steroid hormones in human plasma and urine, Anal. Methods 6:1418−1426

[14] Tolgyesi A, Verebey Z, Sharma VK, Kovacsics L, Fekete J, (2010) Simultaneous determination of corticosteroids, androgens, and progesterone in river water by liquid chromatography-tandem mass spectrometry, Chemosphere 78:972−979

[15] Bahadir EB, Sezginturk MK, (2015) Electrochemical biosensors for hormone analyses, Biosens. Bioelectron. 68:62–71

[16] Carralero V, González-Cortés A, Yánez-Seldeno P, Pingarrón JM, (2007) Nanostructured progesterone immunosensor using a tyrosinase-colloidal gold-graphite-Teflon biosensor as amperometric transducer, Anal. Chim. Acta. 596:86–91

[17] Monrris MJ, Arevalo FJ, Fernandez H, Zon MA, Molina PG, (2012) Integrated electrochemical immunosensor with gold nanoparticles for the determination of progesterone, Sens. Actuators, B. 166–167:586– 592

[18] Trapiella-Alfonso L, Costa-Fernandez JM, Pereiro R, Sanz-Medel S, (2011) Development of a quantum dot-based fluorescent immunoassay for progesterone determination in bovine milk, Biosens. Bioelectron. 26:4753– 4759

383 [19] Kappel ND, Proll F, Gauglitz G, (2007) Development of a TIRF-based biosensor for sensitive detection of
384 progesterone in bovine milk, Biosens. Bioelectron. 22:2295–2300

385 [20] Gillis EH, Traynor I, Gosling JP, Kane MJ, (2006) Improvements to a surface plasmon resonance-based
386 immunoassay for the steroid hormone progesterone, J. AOAC Int. 89:838−842

387 [21] Islam MR, Lu Z, Li X, Sarker AK, Hu L, Choi P, Li X, Hakobyan N, Serpe MJ, (2013) Responsive polymers
388 for analytical applications: a review, Analytica Chimica. Acta. 789:17– 32

389 [22] Islam MR, Gao Y, Li X, Serpe MJ, (2014) Responsive polymers for biosensing and protein delivery, J.
390 Mater. Chem. B, 2:2444-2451

391 [23] Parasuraman D, Serpe MJ, (2011) Poly (*N*-Isopropylacrylamide) microgel-based assemblies for organic
392 dye removal from water, ACS Appl. Mater. Interfaces 3:4714–4721

393 [24] Islam MR, Li X, Smyth K, Serpe MJ, (2013) Polymer-based muscle expansion and contraction, Angew.
394 Chem. 125:10520 –10523

395 [25] Kwon IC, Bae YH, Kim SW, (1991) Electrically erodible polymer gel for controlled release of drugs,
396 Nature 354:291-293

397 [26] Sijbesma RP, Beijer FH, Brunsveld L, Folmer BJ, Hirschberg J, Lange RFM, Lowe JKL, Meijer EW, (1997)
398 Reversible polymers formed from self-complementary monomers using quadruple hydrogen bonding,
399 Science 278:1601-1604

400 [27] Schild HG, (1992) Poly(N-isopropylacrylamide): experiment, theory and application, Progress in
401 Polymer Science, 17:163–249

402 [28] Su S, Ali MM, Filipe CDM, Li Y, Pelton R, (2008) Microgel-based inks for paper-supported biosensing
403 applications, Biomacromolecules, 9:935-941

404 [29] Kim J, Singh N, Lyon LA, (2006) Label-free biosensing with hydrogel microlenses, Angew. Chem., Int. Ed.
405 45:1446–1449

406 [30] Holtz JH, Asher SA, (1997) Polymerized colloidal crystal hydrogel films as intelligent chemical sensing
407 materials, Nature 389:829–832

408 [31] Meng Z, Cho JK, Debord S, Breedveld V, Lyon LA, (2007) Crystallization behavior of soft, attractive
409 microgels, J. Phys. Chem. B 111:6992−6997

410 [32] Sorrell CD, Carter MCD, Serpe MJ, (2011) Color tunable poly (N-Isopropylacrylamide)-co-acrylic acid
411 microgel–Au hybrid assemblies, Adv. Funct. Mater. 21:425−433

412 [33] Sorrell CD, Carter MCD, Serpe MJ, (2011) A “paint-on” protocol for the facile assembly of uniform
413 microgel coatings for color tunable etalon fabrication, ACS Appl. Mater. Interfaces 3:1140–1147

414 [34] Ogino C. Kanehira K, Sasai R, Sonezaki S, Shimizu N, (2007) Recognition and effective degradation of 17
415 β-estradiol by anti-estradiol-antibody-immobilized TiO_2 nanoparticles, J. Biosci. Bioeng. 104:339-342

416 [35] Hoare T, McLean D, (2006) Kinetic prediction of functional group distribution in thermosensitive
417 microgels, J. Phys. Chem. B 110:20327-20336

418 [36] Jones CD, Lyon LA, (2000) Synthesis and characterization of multiresponsive core−shell microgels,
419 Macromolecules 33:8301-8306

420 [37] Hoare T, Pelton R, (2004) Highly pH and temperature responsive microgels functionalized with
421 vinylacetic acid, Macromolecules 37:2544-2550

422 [38] Johnson KCC, Mendez F, Serpe MJ, (2012) Detecting solution pH changes using poly (N-
423 isopropylacrylamide)-co-acrylic acid microgel-based etalon modified quartz crystal microbalances, Analytica
424 Chimica Acta. 739:83-88

425 [39] Carter MCD, Sorrell CD, Serpe MJ, (2011) Deswelling kinetics of color tunable poly(N-
426 Isopropylacrylamide) microgel-based etalons, J. Phys. Chem. B 115:14359-14368

427 [40] Burmistrova A, Richter M, Eisele M, Uzum C, von Klitzing R, (2011) The effect of co-monomer content
428 on the swelling/shrinking and mechanical behaviour of individually adsorbed pNIPAM microgel particles,
429 Polymer 3:1575-1590